Nanoengineering the antibacterial activity of biosynthesized nanoparticles of TiO₂, Ag and Au and their nanohybrids with Portobello mushroom spores (PMS) (TiOx/PMS, Ag/PMS and Au/PMS) and making them optically self-indicating

Iman A. Jaffer Al-Timini and Paul A. Sermon*
Nanomaterials Laboratory, Wolfson Centre, Brunel University, Uxbridge, Middlesex, UB8 3PH, UK
Ahmed A. Burghal, Afrodet A. Salih and Inaam M. N. Alrubaya
Basrah University, College of Science, Iraq

Abstract

Results show that nanoparticles (NPs) can be biosynthesized at room temperature on the reductive and chelating surfaces of Portobello mushroom spores (PMS). Using this green approach TiO_x, Ag, Au, Ag-TiO_x and Au-TiO_x NPs have been prepared. These were characterized by TEM, SIMS and µFTIR-FTIR. TiO_x/PMS, Ag-TiO_x/PMS, Au-TiO_x/PMS and Ag/PMS were active in bacterial inhibition towards *Eschericia coli* and *Staphylococcus aureus*, but Au/PMS was not active (suggesting a strong Au-PMS interaction). TiO_x/PMS, Ag/PMS and Ag-TiO_x/PMS were equally active in an antibacterial and an antifungal sense when tested against *Asperillus* and *Candide*. All samples (except Ag-TiO_x/PMS and Au-TiO_x/PMS) showed an interesting interaction with DNA. We report on the process of fine-tuning these antibacterial properties, progress on making these nanomaterials optically self-indicating and movement towards optical control of their antibacterial activity. Au-TiO_x/PMS shows a surface plasmon resonance (SPR) with a maximum at 518 nm that might be useful in following its anti-bacterial properties (i.e. making the bionanomaterial self-indicating). The future of such green bio-nanomaterials is strong.

Keywords: mushroom, spores, gold, silver, titania, *Eschericia coli*, *Staphylococcus aureus*, *Asperillus, Candide, DNA*

1. Introduction

Nanomaterials are used in bone/tissue engineering [1]. Just as importantly, they are also needed to control infections [2] associated with MRSA, antibiotic-resistant bacteria [3] and multi-drug resistant *Staphylococcus aureus* [4]. Microbial infections have become a global health problem, with antibiotic-resistant genes (ABG) and antibiotic-resistant bacteria (ARB) emerging.

It is well established antimicrobials include 5-40nm Ag nanoparticles (NPs) [4] that may be biosynthesized by green routes from
  (i)   *Chlorella vulgaris* microalgae cells [5]
  (ii)   *Centella asiatica* extract [6]
  (iii) *Arnicae anthodium* extract [7] or
  (iv)   *Phlomis bracteosa* plants [8]
In the last case FTIR showed that the polyphenols were mainly responsible for reduction and capping of synthesized Ag NPs were shown to be formed by their characteristic surface plasmon resonance (SPR) peak at 453 nm and TEM. Biomimetic Ag-oxide nanomaterials [9], nanopatterned surfaces [10] and bio-NP composites [11] are also interesting in an antimicrobial sense, as are bioactive Ti-oxide surfaces [12]. It therefore seemed appropriate to investigate PMS-derived Ag NPs, Au NPs and TiO_x/PMS, Ag/PMS and Au/PMS.

It also seemed suitable to test these against gram positive *Staphylococcus aureus* and gram negative *Escherichia coli* [5,13]; here we wished to measure the diameters of zones of inhibition (mm) on agar plates as previously [8], while also characterizing where the NPs were in relation to the PMS cell wall using TEM [4]. The authors appreciate that anti-microbial strains, that are resistant to conventional anti-microbial agents, have appeared and some agents are unable to access cell membranes, restricting treatment of intracellular pathogens and causing side effects [14,15]. The authors now report a

preliminary study of the antimicrobial and antifungal activity of some green Portobello mushroom spore (PMS)-derived NPs in the hope that work at the bio-nanomaterials interface may prove useful.

2. Antimicrobial Mechanisms

Bacteria can be classified depending on the structure/functional components of the cell wall into:

(i) Gram-positive bacteria (e.g. *Staphylococcus aureus* (*S.aureus*)) whose cell walls contain a thick surrounding layer (20-50 nm) of peptidoglycan (PG) which is attached to specific acids [15] and

(ii) Gram-negative bacteria (e.g. *Escherichia coli (E.coli*)) which is more chemically-structurally complex; here the PG layer is thin and the cell wall tends to be negatively charged [16], with outer membrane containing lipopolysaccharides [15,17].

Anti-bacterial agents can be (a) bactericidal (killing bacteria) and (b) bacteriostatic (slowing bacterial growth [15]). The mechanism of antibiotic resistance may be innate or may involve prevention of the antibiotic from penetrating the bacterial cell wall or hydrolysis/modification/degradation/inactivation of the antibiotic [18,19].

Most anti-microbial agents exhibit inhibition, affect DNA/RNA synthesis, affect the cell membrane or damage the proteins in the cell [14].

With the development of biomedical nanomaterials, safer and alternative anti-microbial agents have started to emerge; these may be unique or may increase the activity of the conventional anti-microbial agents [19]. Treatment strategies include: (i) photo-disinfection with OH· [18], (ii) UV-disinfection at say 264 nm [18], (iii) photo-catalytic disinfection when reactive oxygen species (O_2^-, ·OH or O_2^-) are generated [18] (e.g. with TiO_2/H_2O) [18] and (iv) nanoparticle disinfection. Nanomaterials can be expected to become more important due to their unique chemical [20], mechanical [21], catalytic [22], electrical, magnetic, optical and biological properties [23]. Such properties make NPs powerful tools for vast and diverse applications (e.g. anti-microbial, diagnosis, imaging, and thereby drug delivery (because NPs provide unprecedented opportunities to molecular process and interrogate cellular clinical application [24])). NPs have recently emerged as unique anti-microbial agents due to their shape, size and high surface area to volume ratio; NPs are of the same dimensions as proteins, nucleic acid, membrane of receptors, antibodies and other biomolecules [25].

Antimicrobial NPs [26] operate by mechanisms that are similar (but slightly different due to their different chemical properties, and their size, surface area, shape, crystallinity, charge, surface energy, chemical composition and aggregation [27]). Such NP properties govern their interaction with/in living cells and the way in which they (i) damage or disrupt the integrity of bacterial membrane, (ii) change the microbial cell wall and nucleic basic pathway, (iii) block the enzyme pathway, and (iv) destruct the cell membrane [14]. Conversely, the cytoplasm of Gram-negative bacteria is a strong reducing environment that can affect the oxidation state for metal NPs [26].

Relevant antimicrobial NPs include (i) TiO_2 that have weak mutagenic potential, but are lethal to *S.aureus* and *E.coli* under UVC in 60 min [19,26], (ii) plasmonic Ag and Au that are chemically stable, non-toxic to human cells, biocompatibility [16] and exhibit localized surface plasmon resonance (LSPR) [28] and colour due to the coherent excitation of all free-electrons with the conduction band causing (SPR) an in-phase oscillation [29].

Ag NPs when coated onto a filter for water purification or coated onto medical devices or in dental resin components reduce infection [27] and can be employed in wound healing and can control vector transmitted infection [14] because they react with biomolecules (like DNA, RNA or enzymes during an electron- release mechanism) weakening DNA replication, combine with proteins (causing denaturation and inactivating them by reducing bacterial proteins levels [30]) and interact with P- or S-containing compounds (like DNA leading to damage the cell wall) and may attach to the cell membrane surface and disturb respiration and permeability [17,29]. Au NPs have a large number of atoms available to attach to the surface of bacteria [31,32]. Biosynthesized Au NPs are promising for many medical applications such as anti-tumor, labeling, imaging, apoptosis and interaction with DNA [33]. They also show good biocompatibility, being compatible with human body cells and being resistance to corrosion [34]. Au NPs show a significant anti-bacterial activity depending on their size and shape and also the type of bacteria [24]. They strongly bind to the bacterial cell wall, allowing them to disrupt the bacterial cell membrane, causing leakage of nucleic acids and cytoplasm [17,35], induce photo-mutagenic processes causing damage to DNA and essential proteins [15], increase in ATP (where ATP generation is a significant part in the respiration chain of bacteria via the NAD^+/NADH reaction) intercellular ATP levels, leading to bacterial death and catalyze oxidation reactions, producing ROS that lead to the death of bacteria [35].

Ag-TiO$_x$ and Au-TiO$_x$ nanohybrids show strong anti-microbial activity due to their multi-functionality, e.g. Ag-TiO$_2$ and Au-TiO$_2$ NPs exhibit excellent anti-microbial action [36]. Recently, in green bio routes have been used to synthesis NPs (fungi, bacteria, and plants) [32,33] that may have interesting anti-microbial activity.

3. Experimental

3.1 Materials
Fresh Portobello mushrooms were harvested. Reagents titanium(iv) isopropoxide Ti(OC$_3$H$_7$)$_4$ (ACROS organics; 98%), ethanol (Sigma Aldrich; 99.9%), 2-propanol (Fluka; 99.9%; IPA), AgNO$_3$ (Fisher chemical; >99%), gold (III) chloride hydrate (AuCl$_3$.xH$_2$O; Sigma Aldrich; 99.9%) were used as received. Two bacterial strains (pathogenic) were used during the testing: *Staphylococcus aurous* (Gram positive) and *Escherichia coli* (Gram negative). In addition *Aspergellis* and *candida* were used.

3.2 Instruments
FTIR spectra were recorded on an IR-affinity-1 (Shimadzu) with ATR. μ–FTIR was undertaken on an FT-IR spectrometer (Perkin Elmer, Spotlight 300). Surface morphology and particle size were examined by scanning electron microscopy (SEM, Supra35 VP) with EDX after Pt or Au coating**.** Transmission electron microscopy (TEM, Jeol 2100f, field emission gun (FEG) was used to assess morphology and particle size using a Gatan camera/imaging software (Gatan microscopy suite, version 3). Secondary ion mass spectrometry (SIMS, Kore z-7861-M on a silica wafer) was used to investigate surface composition. Ag, Au and TiO$_2$ nanoparticles were characterized by UV-Vis spectroscopy (Perkin Elmer Lambda 650s).

3.3 Preparations
A 3mM solution of Ti(OC$_3$H$_7$)$_4$ in 5 mL 2-propanol (IPA) was made up and filtered (0.22μm). 4-5 mg Portobello mushroom spores (PMS) were washed twice with water and acetone respectively and were then dispersed in 5 mL water and added with magnetic stirring (1-2h) to give TiO$_x$/PMS.

PMS (4-5mg) was dispersed in 5 mL water (ultrasonic bath for 15 min). At this point, 5 mL of aqueous 3mM AuCl$_3$ solution was added with magnetic stirring at 298K. The pH of the suspensions was 1.4 and adjusted to around 9 - 10 by adding NaOH (0.1 and 0.01M). These Au NP sols were left for 3h under magnetic stirring to give Au/PMS. The colour of the solution changed after 1-3h. The same steps were used to prepare Ag/PMS using 3mM of AgNO$_3$.

Ag-TiO$_x$/PMS nanohybrid was prepared by ultrasonically dispersing 4-5 mg of PMS in 5mL water for 15min. Then, 5mL of aqueous AgNO$_3$ (3mM) were added to the PMS dispersion with magnetic stirring at 298K for 3h. The Ag/PMS was left overnight. Then to 5mL of Ag NPs/PMS was added Ti(OC$_3$H$_7$)$_4$ (3mM) in IPA with magnetic stirring for 3h. The same steps were used to prepare Au-TiO$_x$ NPs/PMS in IPA.

3.4 Bio-activity Measurements
Antibacterial activity was determined in duplicate using Mueller Hinton agar. PMS and NP/PMS samples were dispersed in (and diluted with) IPA or H$_2$O. The antibacterial activity of NPs/PMS was assessed against two pathogenic bacteria species: *Staphylococcus aureus* (Gram positive) and *Escherichia coli* (Gram negative) in the agar well diffusion method. Overnight cultures were used. After 24 h of incubation, bacterial suspension (inoculum) was diluted with sterile physiological solution, for the diffusion test, to 10^8 CFU/mL (colon forming unit) (turbidity = McFarland barium sulfate standard 0.5) [37]. The control sets (IPA and H$_2$O) were maintained at the same condition. The bacterial inoculums were uniformly spread using a sterile cotton swab on a sterile Petri dish containing agar. 50 μL of the PMS or NP/PMS samples were added to each well (6 mm diameter holes cut in the agar gel, 20 mm apart from one another). The plates were incubated for 24 h at 309K, under aerobic conditions. After incubation, confluent bacterial growth was observed. The diameter of the zone of inhibition can be measured in mm [37].

In the agar diffusion disc-variant measurements, NP/PMS were dispersed in (and diluted with) IPA and were used to impregnated 6 mm filter paper discs (Whatman no. 2) to a loading of 10μL or mg.m^{-2}. The discs were maintained at 298K until evaporation was complete and were then kept under refrigeration until the test, when they were placed onto the surface of the agar and incubated overnight at 309 K, at which point the zones of bacterial inhibition were recorded. These measurements were in duplicate [38]. In anti-fungal activity measurements, the NP/PMS samples were assessed against two pathogenic fungi species: *Aspergellis* and *candida* using an agar diffusion disc method. Here the plates were incubated for 72 h at 309 K under aerobic conditions. After incubation, confluent fungi growth was observed. The radii of the regions of inhibition of the fungal growth were again measured (mm); again tests were performed in duplicate [38].

Consideration was also given to PMS and NP/PMS interaction with DNA in a genomic DNA extraction measurement. Nucleic acids from each 200 μL of EDTA-whole blood sample were extracted (after cell lysis and protein denaturation according to the procedure 28) and stored frozen (253K) until required. The concentrations of extracted DNA were measured by NanoDrop ND-1000 spectrophotometer that measured absorbance of DNA, RNA, protein and dye at 220-750 nm [39]. 1.5μL of DNA was assessed at 260nm to determine DNA concentration and the optical density (OD) ratio [39]. To study the effect of/on PMS-based samples on genomic human DNA, 10 μL of each sample was mixed with 10 μL of human genomic DNA. The mixture incubated at 310K for 1 h, then the absorbance of mixture was measured at 260 nm [39] and the DNA concentration was thereby assessed.

4. Characterization Results

4.1 SIMS (see Table 1)
The positive SIMS for PMS and TiO_x/PMS showed some intense peaks. PMS peaks at 28, 45 and 68 m/z are decreased in intensity as a result of TiO_x coating, while peaks at 63 and 64 m/z related to TiO^+ and $TiOH^+$ respectively appeared. The PMS ion fragments need to be related to surface functional groups seen in FTIR (Table 2).

4.2 SEM and TEM
Figures 1-5 illustrate the hollowed oval-shaped morphology of 5μm-sized PMS that was similar to red blood cells and the location of the 10-20nm sized pseudo-spherical discrete Ag and Au NPs and the TiO_x overlayers in the cell walls. The PMS shape is not changed by heating at 373K, apart from an increase on some concave/ convex curvature on fluid loss. When fractured, the cell walls appeared to be ~252 nm thick (i.e. able to accommodate many 10-20nm-sized NPs). Clearly, the Ag and Au NPs were biosynthesized by the functional groups in the PMS cell wall and remain fixed there.

Table 1. Comparison of the intensities of some positive SIMS peaks for the PMS and TiO_x/PMS.

m/z peak	SIMS intensity for PMS	SIMS intensity TiO_x/PMS produced from 0.03mM alkoxide solution	Chemical assignment
15	1200	---	CH_3^+
23	10000	---	Na^+
28	50000	14000	$C_2H_x^+$.
29	15000	---	K^+
40	4000	---	Ca^{2+}
45	7500	2000	$C_2H_5O^+$
63	---	175	TiO^+
65	---	240	TiOH
68	1400	75	$C_xH_yO^+$

Table 2. Functional groups seen in PMS samples with FTIR

Functional group	O-H	N-H	C-H	C=O	C-O	C-N	P-C-O
wavenumber (cm^{-1})	3493	3340	2912-2850	1745,1622	1369	1064	1100

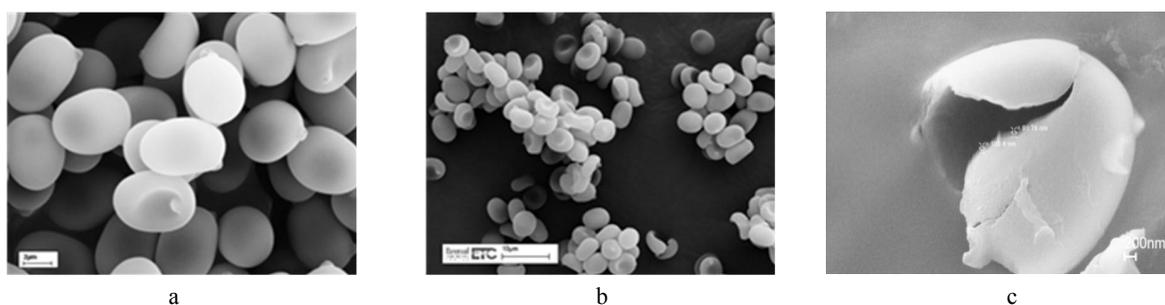a   b   c
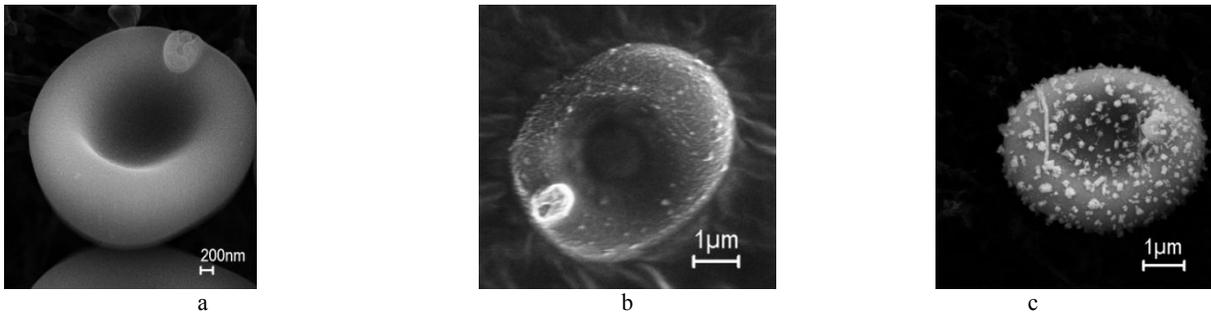Figure 1. SEM of PMS (a) held at 298K (scale bar=2μm), (b) heated at 373K (scale bar=10μm) and (c) fractured PMS

Figure 2. SEM of (a) Au-TiO$_x$/PMS$_{IPA}$, (b) Ag-TiO$_x$/PMS$_{IPA}$ and (c) Au-TiO$_x$/PMS$_{H2O}$
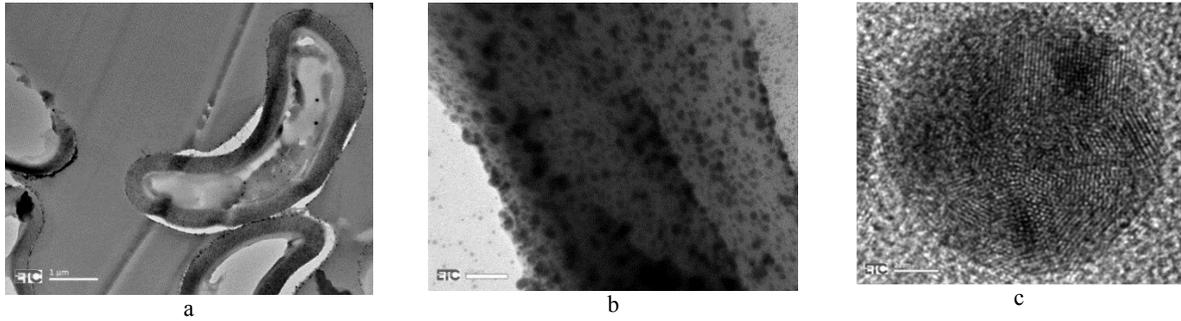

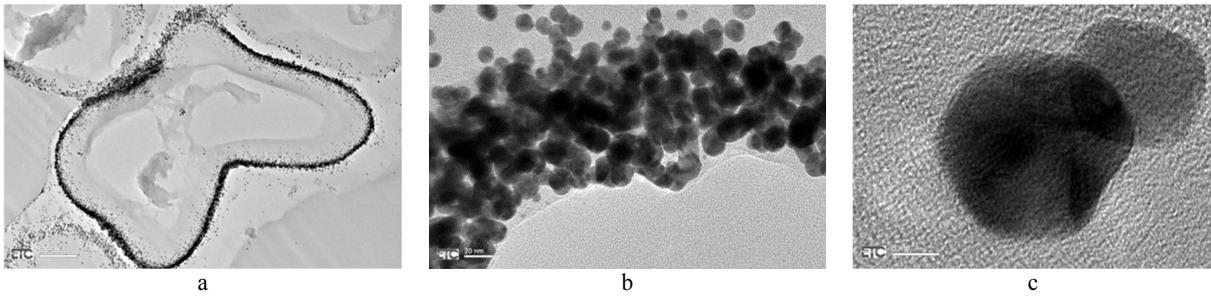Figure 3. TEM of whole Ag/PMS (a), surface of Ag/PMS (b) and Ag NP within the cell wall of Ag/PMS (c)

Figure 4. TEM of whole Au/PMS (a), surface of Au/PMS (b) and Au NP within the cell wall of Au/PMS (c)
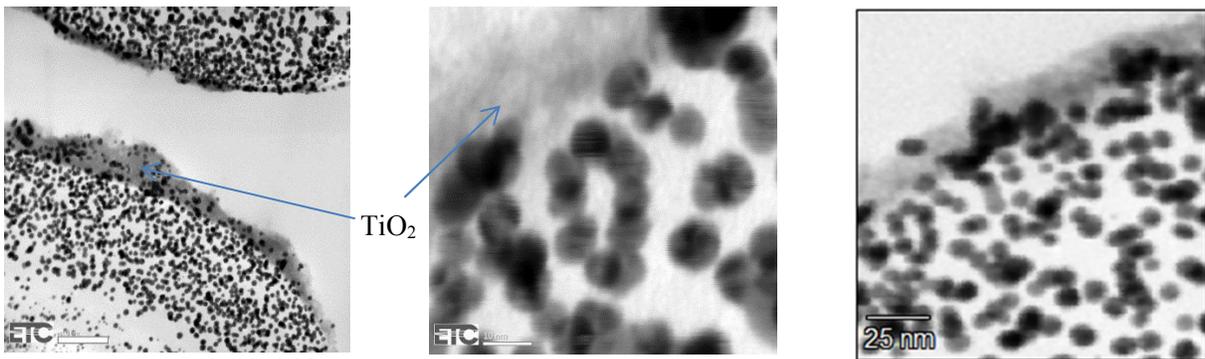

TiO$_2$

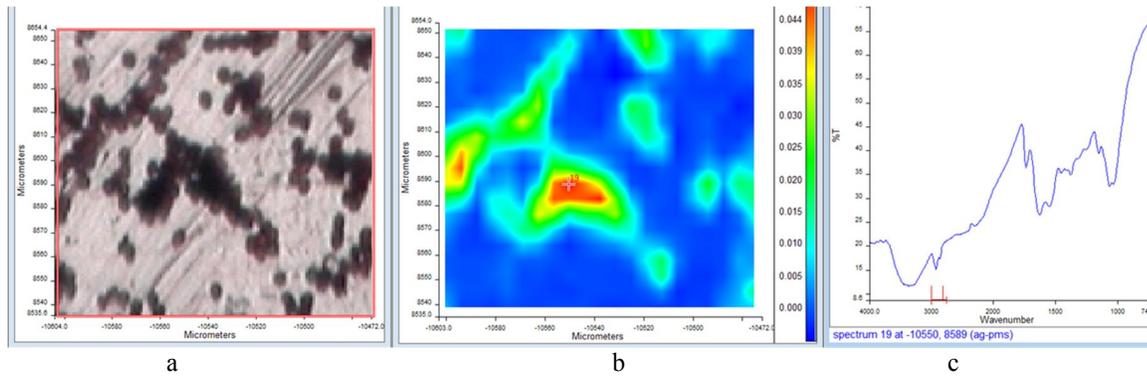Figure 5. TEM of Au NPs and TiO$_x$ layers in the cell walls of Au-TiO$_x$/PMS$_{IPA}$.

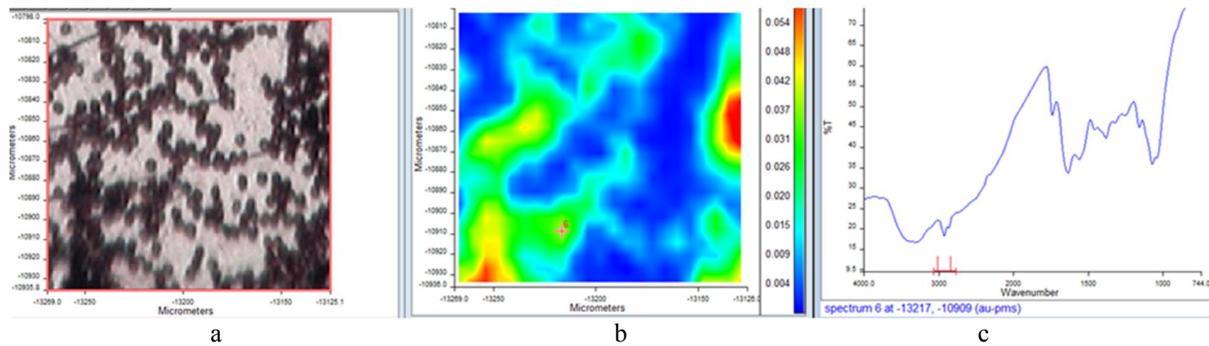Figure 6. Optical image (a) and total absorbance (b) in µFTIR and FTIR (c) for Ag/PMS

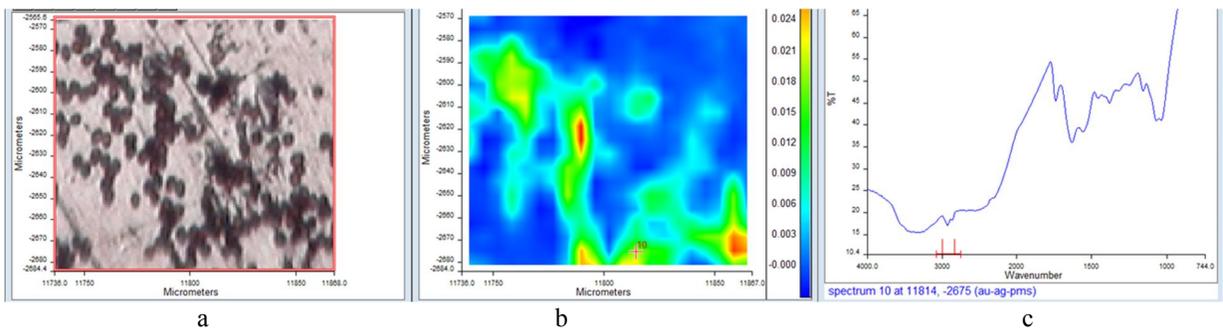Figure 7. Optical image (a) and total absorbance (b) in µFTIR and FTIR (c) for Au/PMS

Figure 8. Optical image (a) and total absorbance (b) in µFTIR and FTIR (c) for Au-Ag/PMS
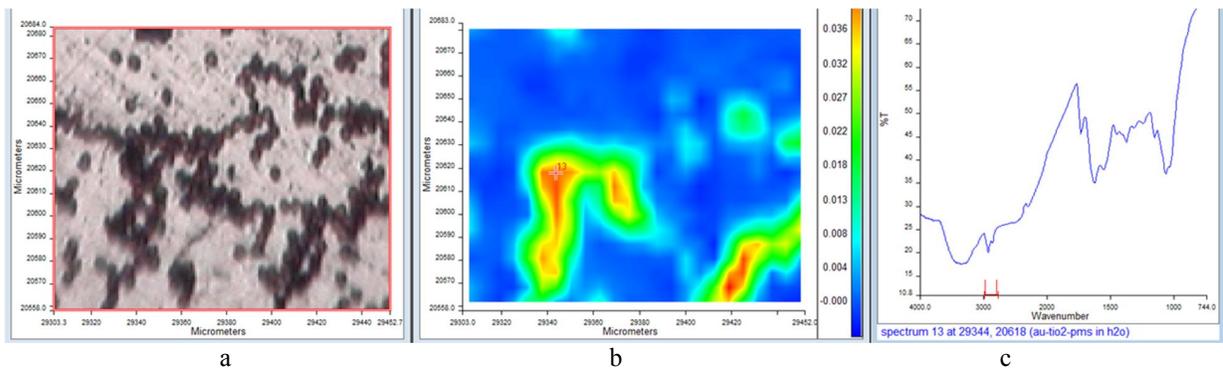

Figure 9. Optical image (a) and total absorbance (b) in µFTIR and FTIR (c) for Au-TiO$_x$/PMS
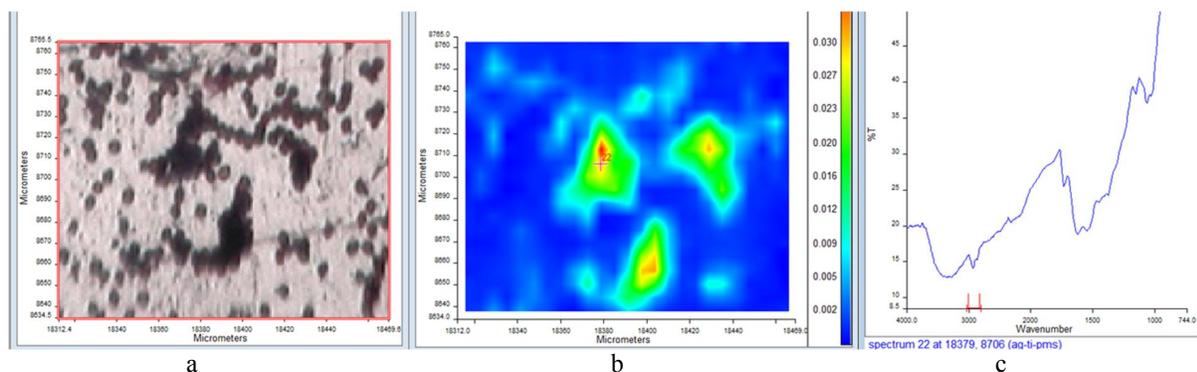
Figure 10. Optical image (a) and total absorbance (b) in µFTIR and FTIR (c) for Ag-TiO$_x$/PMS

4.3 Micro-FTIR (µFTIR) and FTIR (Figures 6-10 and Table 2)

Figure 6-10 show optical images, µFTIR and FTIR of Ag/PMS, Au/PMS, Au-Ag/PMS, Au-TiO$_x$/PMS and Ag-TiO$_x$/PMS. µFTIR allows mapping of chemical functional group mapping in PMS. Figures 6b-10b show some heterogeneity in the total absorbance of microbiological samples (4000-700 cm^{-1}). Figures 6-10c show variations in the absorption bands of hydroxyl, carbonyl and amino groups in FTIR spectra of these samples at 1369 cm^{-1} (C-O) and 1064 cm^{-1} (C-N). These may be responsible for the reduction of the chloroaurate ions (AuCl$_4^-$) and silver ions, along with saccharides, thereby biosynthesizing NPs [40].

5. Anti-microbial and Anti-fungal Activity Results

Tables 3 and 4 show that IPA, Au^{3+}$_{(aq)}$ and Ag$^+$$_{(aq)}$ are active in inhibiting both gram positive (*Staphylococcus aureus*) and gram negative (*Escherichia coli*) bacteria, but not water or PMS alone. At the same time TiO$_x$/PMS, Ag-TiO$_x$/PMS, Au-TiO$_x$/PMS and Ag/PMS in water are active in bacterial inhibition. In contrast, Au/PMS is not at all active. The inference must be that this is because there is a strong Au-PMS interaction arising from ready reduction of Au^{3+}$_{(aq)}$ by the PMS surface. Conversely there can be no free Au^{3+}$_{(aq)}$ after the interaction with dispersed PMS.

Table 5 shows the antibacterial and antifungal activity of five samples produced from a H$_2$O suspension. Again Au/PMS was inactive (as in Table 3). Interestingly, Au-TiO$_x$/PMS was active in inhibiting *E.coli* and *S.aureus*, but not at all active in inhibiting *Asperillus* and *Candide*. TiO$_x$/PMS, Ag/PMS and Ag-TiO$_x$/PMS on the other hand were broadly equally active in an antibacterial and an antifungal sense.

Table 6 shows how five PMS-based samples interacted with human blood DNA at 310K in light and dark conditions after samples had been separated into a PMS-sediment and a supernatant liquid. Data are shown as the % of the absorbance (260nm; A$_{260nm}$) of the added DNA. In almost all supernatant liquid samples and PMS sediment samples (in light and dark conditions), A$_{260nm}$ increased greatly beyond the level of the DNA added initially. The only samples that did not show this effect in the supernatant liquid were Ag-TiO$_x$/PMS and Au-TiO$_x$/PMS, but even then the PMS sediment did show an elevated A$_{260nm}$.

Table 3. Diameter (mm) of inhibition activity against *E.coli* and *S.aureus* by holes samples (9 mm diameter)

	controls			NPs/PMS in IPA			NPs/PMS in H$_2$O		
	H$_2$O	IPA	PMS	TiO$_x$ /PMS	Ag -TiO$_x$ /PMS	Au -TiO$_x$ /PMS	Au^o /PMS	Ag^o /PMS	Au^o-Ag^o /PMS
E.coli	0	15	0	15	16	20	0	13	11
S.aureus	0	13	0	18	17	17	0	15	12
NP or PMS concn (mg/100µL)	-	-	4	0.016	0.01/0.007	0.01/0.01	0.039	0.021	-

Table 4. Diameter (mm) of inhibition activity of precursor salts and ions Au against *E.coli* and *S.aureus* (9 mm diameter)
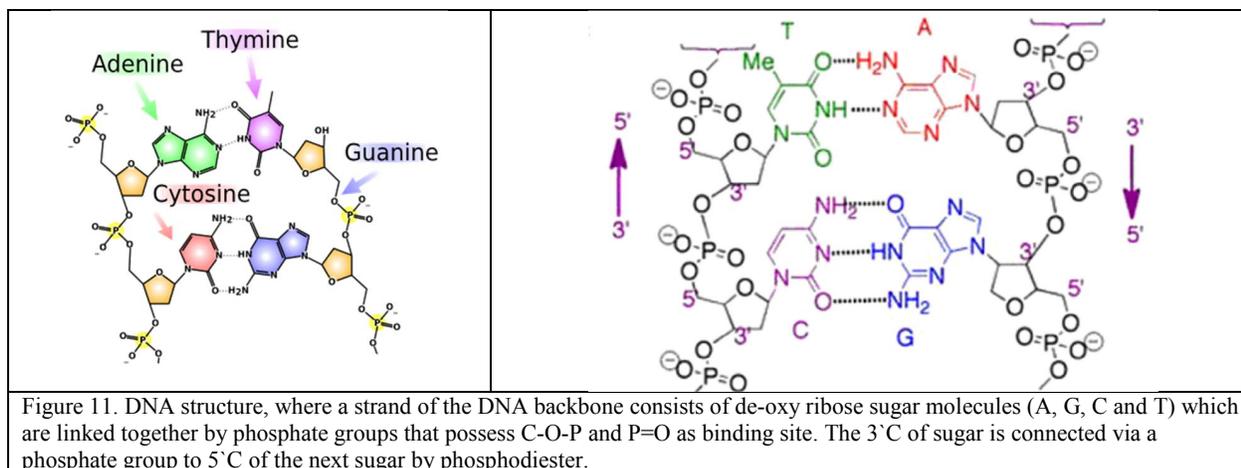
	salts in IPA			salts in H$_2$O		
	Au^{3+}	Ti^{4+}	Ag$^+$	Ag$^+$	Au^{3+}	
E.coli	19	19	24	14	15	
S.aureus	28	22	24.	16	17	
Salt or ion concn (mg/100μL)	3.05	2.55	0.05	0.05	3.05	

Table 5. Diameter (mm) of inhibition activity (6mm diameter) of samples dispersed in H$_2$O

	TiO$_x$ /PMS 8μg/50μL	Ag-TiO$_x$ /PMS 13-21 μg/50μL	Au-TiO$_x$ /PMS 42-130 μg/50μL	Au/ PMS 25 μg/50μL	Ag/ PMS 13μg/50μL
E.coli	9-7	10-9	8-9	0.00	9-11
S.aureus	20	8-10	7-7	0.00	9-8
Aspergillus	7	8	0.00	0.00	7-9
Candide	11	9-7	0.00	0.00	11-12

Table 6. Effect (%) on original human blood DNA in the light and dark in supernatant liquid about PMS samples and in PMS precipitates

	TiO$_x$ /PMS	Ag/ PMS	Au/ PMS	Ag-TiO$_x$ /PMS	Au-TiO$_x$ /PMS
Supernatant liquid/Dark	1048	133	216	89	50
PMS sediment/Dark	1278	214	294	229	460
Supernatant liquid/Light	659		228	659	194
PMS sediment/Light	917			229	1622

Figure 11. DNA structure, where a strand of the DNA backbone consists of de-oxy ribose sugar molecules (A, G, C and T) which are linked together by phosphate groups that possess C-O-P and P=O as binding site. The 3`C of sugar is connected via a phosphate group to 5`C of the next sugar by phosphodiester.

6. Discussion and Conclusions

The biosynthesis of NPs/PMS can be explained by an important factor: the nicotinamide adenine dinucleotide NADH and NADH dependent enzyme. The reduction appears to be started by electron transfer as an electron carrier from NADH-dependent enzyme. This process may play a key role in the biosynthesis and bio-transformation reactions [32]. The mechanism of formation of NPs/PMS may involve trapping of Ag or Au ions on the surface of PMS and electrostatic interaction between the positive charge of ions and negative charge of carboxylic and hydroxyl groups on the cell wall of PMS in basic solution [41]. Furthermore, PMS involves many functional groups and active compounds that can be reacted as both a reducing and capping agent [32] (NADH →NAD$^+$ + e$^-$). Proteins and polysacchrides play an important role in any reaction with metal ions, because of the COO$^-$ and O-H groups which have a strong ability to chelate/react with Ag and Au ions. PMS contain many functional groups. For example, glucose has carbonyl groups which are highly polar (C$^+$-O$^-$) and namely an aldehyde.

This structure is flat (trigonal) and it can be that hydroxyl ions attack the carbonyl group. The mechanism of reaction in an alkaline environment (pH ≥ 10) occurs according to: $2Ag^+ + -CH_2OH$ (glucose) $+ 3OH^- \rightarrow 2Ag^o + -C=O + H_2O$ or $Ag^+ + -CH_2OH$ (glucose) $+ OH^- \rightarrow 2Ag^o + -COOH + 1/2 H_2$. It is known that edible mushroom consists of 75% proteins [42]. For example, carbonyl group in amino acid, peptides of proteins, enzyme and polysaccharide might have a strong ability to bind with silver and play a role in the reduction of metal ions to atoms by the oxidation of aldehyde group to carboxylic acid [43]. So, the proteins probably can form a layer on the Ag or Au NPs which prevents agglomeration of NPs. Therefore, the NPs are stabilized in the mixture [44].

Ag-TiO$_x$/PMS is active against an antimicrobial and an antifungal agent, but Au-TiO$_x$/PMS is only active against bacteria. This again may reflect on the strength of the Au-PMS interaction. One would expect that NPs/PMS would bind through several metals ions or atoms in the microbial cell [24].

The properties of the bacteria cell wall can play a crucial role in different NPs/PMS because the wall is designed to provide rigidity, shape and strength to protect the cell from osmotic rupture. Gram positive bacteria were found to be more susceptible to the NPs/PMS than Gram negative bacteria because of the difference in their cell wall structure. Gram negative bacteria are considered to be more resistant due to their outer membrane acting as a barrier to many environmental substances including antibiotics [15]. In addition, the charge on the membrane of *E.coli* is negative because of the excess number of carboxyl groups, which upon dissociation makes the cell surface negative. The opposite charges of bacteria and nanoparticles are attributed to their bioactivity due to electrostatic forces leading to electrical interaction between the *E.coli* and NPs/PMS increasing the possibility of collisions and decreasing the bacteria growth [17].

Moreover, increasing the surface area/decreasing the particle size, could be helping to improve NP anti-microbial activity [24]. NPs have a large surface area available for interaction, which enhance the bactericidal effect more than the large sized particles; hence they impart cytotoxicity to the microorganisms. However, the aggregation of NPs leads to decreasing the property of the interaction of NPs with bacteria cells [17]. The size of NPs can give rise to electronic effects which promote their surface reactivity and prevent the aggregation of NPs. For example, NPs with diameter less than 10 nm have anti-microbial activity but NPs with diameter 30-50 nm did not have good anti-microbial activity until NPs reached 20 μg/mL [24].

TiO$_x$ NPs/PMS and monohybrid have good anti-bacterial activity against *E.coli*. When the cell of bacteria absorbs the NPs significant oxidative stress happens due to the generation of free radicals like ·OH, O$_2^-$ and H$_2$O$_2$ by oxidation of poly unsaturated phospholipids. Hence, these lipids started to submit a peroxidation reaction subsequently leading to:
- glutathione (GSH) depletion
- stress or eventual disruption in the morphology of cell membrane, and
- the electron transfer leading to cellular death [34].

Ag NPs/PMS and monohybrid have excellent anti-bacterial activity against both *E.coli* and *S.aureus* due to the generation of ROS following the administration of NPs. Our results show that Ag NPs/PMS have anti-bacterial activity in lower concentration than other NPs. High activity of silver NPs is attributed to species difference as they dissolve to release Ag^0, Au^0, Ag$^+$, Au$^+$ clusters. Several mechanisms have been suggested leading to the inhibition of bacteria growth:
- Binding Ag NPs with proteins or lipo-poly-saccharide in the cell membrane leading to collapse [15].
- Ag NPs were found to induce phosphate and interaction with atoms which have a high electron density like S, O and N. These are essential biological molecules as thiol group because Ag NPs have an extreme chemical affinity for sulfur group. The interaction with thiol or cysteine in protein leads to denaturation effects, loss of the subsequent of enzyme and changing cytoplasmic components [34].
- Attacking the respiratory chain and inhibition of the respiratory enzymes with the division of cells and causing death [17].
- Starting to act on dehydrogenases of electron transport and reduction of cellular adenosine triphosphate (ATP) level.

Interestingly, Au NPs/PMS do not have any bacterial activity. It can be suggested that:
- Au NPs self-assemble in 4-5 μm long PMS indicating a strong NP-PMS interaction [27].
- Au NPs aggregation caused a decreased inhibitory effect; increasing surface area generates further biophysical interactions [17]
- Au NPs /PMS may be absorbed only on the cell of bacteria but cannot penetrate inside bacteria cells [24].

The ability of biomolecules (like nucleic acid and proteins) to chelate [34] and adsorb [35] Au NPs may direct the NPs to specific sites [34] or change their biological effects [35]. Nevertheless, Au NPs are particularly attractive for target direction diagnostics and therapeutics in the human body [34].

The potent anti-fungal of TiO_x/PMS is the most effective catalyst for chemical transformation [35].

Present data suggests that Ag/PMS has a potential as a biocide against *Aspergillus* and *Candide*. Indeed, the disrupting of the structure cell membrane and inhibiting the normal budding process is due to the damage of the membrane integrity [28]. 16).

The results of the present study support the suggestion plant-derived NPs have antibacterial properties that can be utilized as antibacterial agents in new drugs for the therapy of infectious disease caused by pathogens [44].

In addition PMS-based nanomaterials clearly interact with DNA. Figure 11 illustrates the structure of DNA. The base pairs of DNA possess strong absorbance at 260 nm [45]; if the DNA helix is denatured, base stacking is destroyed and UV absorbance goes up. The effect of PMS and most NP/PMS samples was to increase absorbance at 260nm above that for the DNA introduced (both in light and dark conditions and in the supernatant and PMS sediment). The only exception was for the supernatant liquid of Ag-TiO_x/PMS$_{(H2O, IPA)}$ and Au-TiO_x/PMS$_{(H2O, IPA)}$. One assumes that all other samples lower base stacking, blocking of DNA replication and causing DNA damage [41]. Figure 12 shows that the absorbance changes in the form of hyperchromism and hypochromism. The present results appear to show that hyperchromism occurs suggesting breakage of the DNA structure. That means a strong interaction between TiO_x NPs/PMS and nanohybrid with DNA.
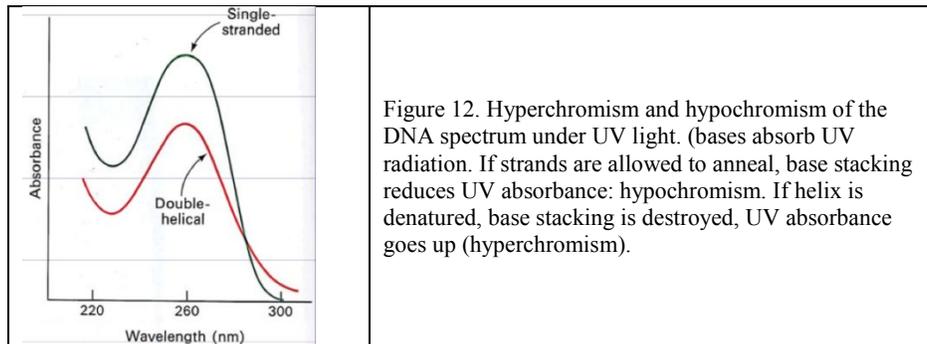

Figure 12. Hyperchromism and hypochromism of the DNA spectrum under UV light. (bases absorb UV radiation. If strands are allowed to anneal, base stacking reduces UV absorbance: hypochromism. If helix is denatured, base stacking is destroyed, UV absorbance goes up (hyperchromism).

Electrostatic interactions can change the conformation/structure of DNA. For example, H-bonds, hydrophobic effect and stacking interactions between complementary bases hold the two strands of DNA together. When NPs/PMS were added, the base-base interaction was reduced in the DNA structure, owing to many bases becoming free form and H-bond breakage leading to an increase absorbance [45]. Furthermore, the presence of a single stranded DNA will be higher than double stranded DNA in the same concentration.

Moreover, the mechanism of reaction can occur by the phosphate group of DNA which has a negative charge. The positive charge of metals can bind to P=O to form P-O-M via electrostatic reaction [46]. From the results we can see that there are future applications for using these materials as anticancer drugs by destroying the nuclear materials for the tumour cells.

Ag NPs appear to enter the cell and intercalate between the purine and pyrimidine base pars disrupting the hydrogen bonding between the two anti-parallel strands and denaturing the DNA molecule [47].

In general, all samples can analyze DNA in dark and light. NPs/PMS in mixture and precipitate have an excellent effect which reaches 60 ng/μL. In contrast, NPs/PMS monohybrid supernatant show some decrease in absorbance due to lower NPs/PMS concentration [32]. Explain why DNA was not from PMS.

The interaction between TiO_x NPs/PMS and monohybrid with human DNA under UV can be explained via the covalent interaction and non-covalent interaction. First, NP/PMS hybrids can bind to alkylation or intra and inter strand crosslinking of DNA as a covalent interaction. Secondly, the non-covalent interaction leads to DNA strands breakage, changing DNA conformation or torsional tension [43]. Additionally, non-covalent interaction involves the following:

- TiO$_x$/PMS and hybrids could be interacting between bases pairs.
- they bind to a sugar phosphate group's backbone or the major or minor groove.
- The electrostatic interaction of these NPs includes binding to the exterior of the helix by non-covalent interaction [45].

Several hypotheses can be suggested to explain the increase in absorbance at 260 nm:
  (i)   Exposure of the bases' purine and pyrimidine of DNA when NPs interact with DNA leading to a slight change in the human DNA conformation and
  (ii) NPs release ROS causing DNA damage [48].

Optical amplifiers (e.g. liquid crystals) have been reported [49] to be useful for detection of gram-positive and gram negative bacteria. The authors are considering whether their Au-Ag/TiO$_x$ bionanomaterials also have useful optical properties. Conversely, UV promotes antibacterial effects in TiO$_2$ nanocomposites even after cessation of UV irradiation [50].
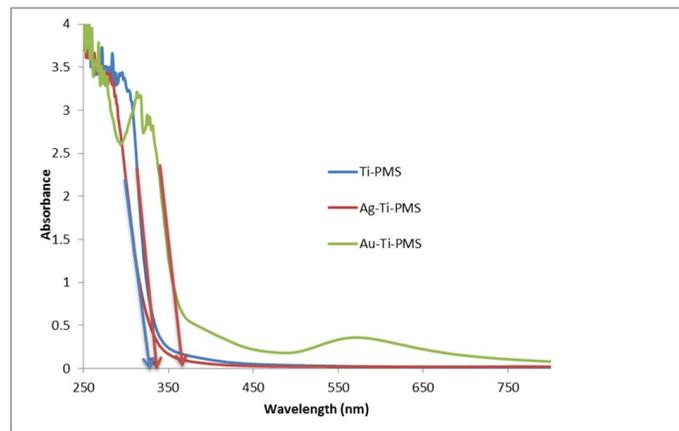

Figure 13. UV-Vis absorbance spectra of TiO$_x$ NPs/PMS and their monohybrids.

Figure 13 shows that Au-TiO$_x$/PMS shows a surface plasmon resonance (SPR) with a maximum at 518 nm, confirming the presence of Au NPs seen in TEM, and this might be used to follow its antibacterial activity, making this nanomaterial self-indicating.

7. Acknowledgements

8. References

[1]   Dhivya, S., Ajita, J. and Selvamurugan, N. 'Metallic nanomaterials for bone tissue engineering' J.Biomed.Nanotech. 11,1675-1700 (2015)

[2]   Schierholz, J.M. and Beuth, J. 'Implant infections: a haven for opportunistic bacteria' J.Hosp.Infect. 49, 87-93, (2001)

[3]   Wang, F. et al 'Nanoparticle-based antivirulence vaccine for the management of methicillin-resistant Staphylococcus aureus skin infection' Adv.Funct.Mater. 26,1628-1635 (2016)

[4]   Manikprabhu, D. et al 'Sunlight mediated synthesis of silver nanoparticles by a novel actinobacterium (Sinomonas mesophila MPKL 26) and its antimicrobial activity against multi drug resistant Staphylococcus aureus' J.Photochem.Photobiol. 158B,202-205 (2016)

[5]   Ebrahiminezhad, A., Bagheri, M., Taghizadeh, S.M., Berenjian, A. and Ghasemi, Y. 'Biomimetic synthesis of silver nanoparticles using microalgal secretory carbohydrates as a novel anticancer and antimicrobial' Adv.Nat.Sci.Nanosci.nanotechnol. 7,AR 015018 (2016)

[6]   Netala, V.R. et al 'First report of biomimetic synthesis of silver nanoparticles using aqueous callus extract of Centella asiatica and their antimicrobial activity' Appl.Nanosci. 5,801-807 (2015)

[7]   Dobrucka, R. and Dlugaszewska, J. 'Antimicrobial activities of silver nanoparticles synthesized by using water extract of Arnicae anthodium Ind.J.Microbiol. 55,168-174 (2015)

[8]   Anjum, S. and Abbasi, B.H. 'Biomimetic synthesis of antimicrobial silver nanoparticles using in vitro-propagated plantlets of a medicinally important endangered species: Phlomis bracteosa' Internat.J.Nanomed. 11,1663-1675 (2016)

[9]   Manna, J., Goswami, S., Shilpa, N., Sahu, N. and Rana, R.K. 'Biomimetic method to assemble nanostructured Ag@ZnO on cotton fabrics: Application as self-cleaning flexible materials with visible-light photocatalysis and antibacterial activities' ACS Appl.Mater.Interf. 7,8076-8082 (2015)

[10] Dickson, K.N., Liang, E.I., Rodriguez, L.A., Vollereaux, N. and Yee, A.F. 'Nanopatterned polymer surfaces with bactericidal properties' Biointerphas. 10,AR 021010 (2015)

[11] Jackson, E. et al 'Protein-templated biomimetic silica nanoparticles' Lang. 31,3687-3695 (2015)

[12] Cai, X.Y., Li, N.N., Chen, J.C., Kang, E.T. and Xu, L.Q. 'Biomimetic anchors applied to the host-guest antifouling functionalization of titanium substrates' J.Coll.Interf.Sci. 475,8-16 (2016)

[13] Rathore, H.S. et al 'Fabrication of biomimetic porous novel sponge from gum kondagogu for wound dressing' Mater.Lett. 177,108-111 (2016)

[14] Yah, C.S. and Simate, G.S. 'Nanoparticles as potential new generation broad spectrum antimicrobial agents.' Daru 23,(1),43- (2015)

[15] Hajipour, M.J. et al 'Antibacterial properties of nanoparticles' Trends Biotechnol. 30,499–511 (2012)

[16] Bankura, K., et al 'Antibacterial activity of Ag-Au alloy NPs and chemical sensor property of Au NPs synthesized by dextran' Carbohydr.Polym. 107,151–157 (2014)

[17] Chen, S.F. et al 'Large scale photochemical synthesis of M@TiO$_2$ nanocomposites (M = Ag, Pd, Au, Pt) and their optical properties, CO oxidation performance, and antibacterial effect' Nano.Res. vol?,1–12 (2010)

[18] Sharma, V.K., Johnson, N., Cizmas, L., McDonald, T.J. and Kim, H. 'A review of the influence of treatment strategies on antibiotic resistant bacteria and antibiotic resistance genes' Chemosphere 150,702–714 (2016)

[19] Wright, G.D. 'Molecular mechanisms of antibiotic resistance' Chem.Commun. 47,4055- (2011)

[20] Bindhu, M.R. and Umadevi, M. 'Antibacterial activities of green synthesized gold nanoparticles' Mater. Lett. 120,122–125 (2014)

[21] Muthuvel, A., Adavallan, K., Balamurugan, K. and Krishnakumar, N. 'Biosynthesis of gold nanoparticles using Solanum nigrum leaf extract and screening their free radical scavenging and antibacterial properties' Biomed.Prev.Nutr. 4,325–332 (2014)

[22] Brayner, R. 'The toxicological impact of nanoparticles' Nano.Today 3,48–55 (2008)

[23] Giner-Casares, J.J., Henriksen-Lacey, M., Coronado-Puchau, M. and Liz-Marzán, L.M. 'Inorganic nanoparticles for biomedicine: Where materials scientists meet medical research' Mater.Today 19,page- (2015)

[24] Eiampongpaiboon, T., Chung, W.O., Bryers, J.D., Chung, K-H. and Chan, D.C.N. 'Antibacterial activity of gold-titanates on Gram-positive cariogenic bacteria' Acta Biomater.Odontol.Scand. 1,51–58 (2015)

[25] Dinakar, S., Isacc Fenn Fenn, R., Sobczak-Kupiec, A. and Basavegowda, N. 'Bioreduction of chloroaurate ions using fruit extract Punica granatum (Pomegranate) for synthesis of highly stable gold nanoparticles and assessment of its antibacterial activity' Micro.Nano.Lett. 8,400–404 (2013)

[26] Lemire, J.A., Harrison, J.J. and Turner, R.J. 'Antimicrobial activity of metals: mechanisms, molecular targets and applications.' Nat.Rev.Microbiol. 11,371–84 (2013)

[27] Zhou, Y., Kong, Y., Kundu, S., Cirillo, J.D. and Liang, H. 'Antibacterial activities of gold and silver nanoparticles against Escherichia coli and bacillus Calmette-Guérin.' J.Nanobiotechnol. 10,19- (2012)

[28] Tran, Q.H., Nguyen, V.Q. and Le, A.T. 'Silver nanoparticles: synthesis, properties, toxicology, applications and perspectives' Adv.Nat.Sci.Nanosci.Nanotechnol. 4,033001 (2013)

[29] Sharma, V.K., Yngard, R.A. and Lin, Y. 'Silver nanoparticles: green synthesis and their antimicrobial activities' Adv.Coll.Interf.Sci. 145,83–96 (2009)

[30] Guzman, M., Dille, J. and Godet, S. 'Synthesis and antibacterial activity of silver nanoparticles against gram-positive and gram-negative bacteria' Nanomed.Nanotechnol.Biol.Med. 8,(1),37–45 (2012)

[31] Zhang, Y., Peng, H., Huang, W., Zhou, Y. and Yan, D. 'Facile preparation and characterization of highly antimicrobial colloid Ag or Au nanoparticles' J.Coll.Interf.Sci. 325,371–376 (2008)

[32] Sadhasivam, S., Shanmugam, P., Veerapandian, M., Subbiah, R. and Yun, K. 'Biogenic synthesis of multidimensional gold nanoparticles assisted by Streptomyces hygroscopicus and its electrochemical and antibacterial properties' BioMetals 25,351–360 (2012)

[33] Koperuncholan, M. 'Bioreduction of chloroauric acid (HAuCl$_4$) for the synthesis of gold nanoparticles (GNPs): A special empathies of pharmacological activity' Int.J.Phytopharm. 5,72–80 (2015)

[34] Chapman, F.R.J. and Sullivan, T. Nanoparticles in anti-microbial materials: Use and characterisation. RSC Nanosci.Nanotechnol. 2012.

[35] Zhao, Y., Ye, C., Liu, W., Chen, R. and Jiang, X. 'Tuning the composition of AuPt bimetallic nanoparticles for antibacterial application' Angew.Chemie Int.Ed. 53,8127–8131 (2014)

[36] Kholmanov, I.N. et al 'Nanostructured hybrid transparent conductive films with antibacterial properties' ACS Nano 6,5157–5163 (2012)

[37] Smania, A., Monache, F.D., Smania, E. de F. A. and Cuneo, R.S. 'Antibacterial activity of steroidal compounds isolated from Ganoderma applanatum (Pers.) Pat. (Aphyllophoromycetideae) fruit body' Int.J.Med.Mushrooms 1,325–330 (1999)

[38] Vanden Berghe, D.A. and Vlietinck, A.J. 'Screening methods for antibacterial and antiviral agents from higher plants' 6,47–69 (Jan. 1991)

[39] Sambrood, J.J., Fritsch, E.F. and Maniatis, T., Molecular cloning: A laboratory manual. Cold Spring Harbor Laboratory PressNo Title, 1989.

[40] Huang, J. et al 'Biogenic silver nanoparticles by Cacumen platycladi extract: synthesis, formation mechanism, and antibacterial activity' Ind.Eng.Chem.Res. 50,9095–9106 (2011)

[41] Sadowski, Z. 'Biosynthesis and application of silver and gold nanoparticles, silver nanoparticles.' Intech Open, 257–277 (2010)

[42] Bhat, R., Deshpande, R., Ganachari, S.V., Huh, D.S. and Venkataraman, A. 'Photo-irradiated biosynthesis of silver nanoparticles using edible mushroom Pleurotus florida and their antibacterial activity studies' Bioinorg.Chem.Appl. , 7pages, 2011.

[43] Sirajuddin, M., Ali, S. and Badshah, A. 'Drug-DNA interactions and their study by UV-Visible, fluorescence spectroscopies and cyclic voltametry' J.Photochem.Photobiol. 124B,1–19 (2013)

[44] Anthony, K.J.P., Murugan, M., Jeyaraj, M., Rathinam, N.K. and Sangiliyandi, G. 'Synthesis of silver nanoparticles using pine mushroom extract: A potential antimicrobial agent against E. coli and B. subtilis' J.Ind.Eng.Chem. 20,2325–2331 (2013)

[45] Suhani Patel, S.B., et al 'DNA binding and dispersion activities of titanium dioxide nanoparticles with UV/vis spectrophotometry, fluorescence spectroscopy and physicochemical analysis at physiological temperature' Mol. Liq. 213,304–311 (2016)

[46] Jin, C., et al 'In vivo evaluation of the interaction between titanium dioxide nanoparticle and rat liver DNA.' Toxicol.Ind.Health 29,235–44 (2013)

[47] Klueh, U., Wagner, V., Kelly, S., Johnson, A. and Bryers, J.D. 'Efficacy of silver-coated fabric to prevent bacterial colonization and subsequent device-based biofilm formation' J. Biomed.Mater.Res. 53,621–631 (2000)

[48] El-Said, K., Ali, E., Kanehira, K. and Taniguchi, A. 'Molecular mechanism of DNA damage induced by titanium dioxide nanoparticles in toll-like receptor 3 or 4 expressing human hepatocarcinoma cell lines' J. Nanobiotechnol. 12,(1),48- (2014)

[49] Zafiu, C. et al 'Liquid crystals as optical amplifiers for bacterial detection' Biosens.Bioelectron. 80,161-170 (2016)

[50] Cai, Y., Strømme, M. and Welch, K. 'Photocatalytic antibacterial effects are maintained on resin-based TiO_2 nanocomposites after cessation of UV irradiation' PLoS One 8,10- (2013)